

## Characterization and regulation of T-type $\text{Ca}^{2+}$ channels in embryonic stem cell-derived cardiomyocytes

Ying Ming Zhang,<sup>1\*</sup> Lijuan Shang,<sup>1\*</sup> Criss Hartzell,<sup>2</sup> Michael Narlow,<sup>1</sup> Leanne Cribbs,<sup>3</sup> and Samuel C. Dudley, Jr.<sup>1</sup>

<sup>1</sup>Division of Cardiology, Atlanta Veterans Affairs Medical Center, Decatur 30033;

<sup>2</sup>Department of Cell Biology, Emory University, Atlanta, Georgia 30322; and <sup>3</sup>Department of Medicine, Cardiovascular Institute, Loyola University Medical Center, Maywood, Illinois 60153

Submitted 27 December 2002; accepted in final form 6 August 2003

**Zhang, Ying Ming, Lijuan Shang, Criss Hartzell, Michael Narlow, Leanne Cribbs, and Samuel C. Dudley, Jr.** Characterization and regulation of T-type  $\text{Ca}^{2+}$  channels in embryonic stem cell-derived cardiomyocytes. *Am J Physiol Heart Circ Physiol* 285: H2770–H2779, 2003. First published August 14, 2003; 10.1152/ajpheart.01114.2002.—T-type  $\text{Ca}^{2+}$  channels may play a role in cardiac development. We studied the developmental regulation of the T-type currents ( $I_{\text{Ca,T}}$ ) in cardiomyocytes (CMs) derived from mouse embryonic stem cells (ESCs).  $I_{\text{Ca,T}}$  was studied in isolated CMs by whole cell patch clamp. Subsequently, CMs were identified by the myosin light chain 2v-driven green fluorescent protein expression, and laser capture microdissection was used to isolate total RNA from groups of cells at various developmental time points.  $I_{\text{Ca,T}}$  showed characteristics of  $\text{Ca}_v3.1$ , such as resistance to  $\text{Ni}^{2+}$  block, and a transient increase during development, correlating with measures of spontaneous electrical activity. Real-time RT-PCR showed that  $\text{Ca}_v3.1$  mRNA abundance correlated ( $r^2 = 0.81$ ) with  $I_{\text{Ca,T}}$ . The mRNA copy number was low at 7+4 days (2 copies/cell), increased significantly by 7+10 days (27/cell;  $P < 0.01$ ), peaked at 7+16 days (174/cell), and declined significantly at 7+27 days (25/cell). These data suggest that  $I_{\text{Ca,T}}$  is developmentally regulated at the level of mRNA abundance and that this regulation parallels measures of pacemaker activity, suggesting that  $I_{\text{Ca,T}}$  might play a role in the spontaneous contractions during CM development.

growth and development; gene expression regulation; biological pacemaker; ion channel

IN CARDIAC TISSUE, two types of inward  $\text{Ca}^{2+}$  channels, L- and T-type channels, have been identified. L-type  $\text{Ca}^{2+}$  channels have a relatively large conductance, are activated at depolarized potentials, and have been thought to contribute most of the  $\text{Ca}^{2+}$  required for  $\text{Ca}^{2+}$ -induced  $\text{Ca}^{2+}$  release during excitation-contraction coupling. On the other hand, the role of the low voltage-activated T-type  $\text{Ca}^{2+}$  channels has not been well understood. Some studies suggest that T-type  $\text{Ca}^{2+}$  channels may play a role in cardiac pacemaker activity because they are abundant in nodal tissue (5) and activated in a voltage range consistent with pacemaker

activity (5, 37). Also, T-type channels may be involved in cardiac development, possibly indicating a link between spontaneous activity and cardiac differentiation. They have been observed at a higher density in embryonic and neonatal myocytes (11, 16, 20) than in mature ventricular myocytes (16, 20). Complicating the study of T-type  $\text{Ca}^{2+}$  currents ( $I_{\text{Ca,T}}$ ) has been the observation that despite the presence of  $\text{Ca}_v3$  transcript,  $I_{\text{Ca,T}}$  has been easier to record in smaller mammals than in adult human tissue (21). This may be the result of downregulation of  $I_{\text{Ca,T}}$  during human development (25).

T-type channels are encoded by at least three genes:  $\text{Ca}_v3.1$  ( $\alpha 1\text{G}$ ),  $\text{Ca}_v3.2$  ( $\alpha 1\text{H}$ ), and  $\text{Ca}_v3.3$  ( $\alpha 1\text{I}$ ). Northern blotting results have shown that transcripts of  $\text{Ca}_v3.1$  and  $\text{Ca}_v3.2$  are found in the adult human heart (2, 22). In the neonatal rat and fetal mouse heart, data strongly suggest that  $\text{Ca}_v3.1$  encodes the cardiac T-type channel (3, 16).  $\text{Ca}_v3.3$  mRNA has been found primarily in the brain and has not been detected in the heart (14, 16).

Mouse pluripotent embryonic stem cells (ESCs) retain their developmental capacity and can be differentiated in vitro into cardiomyocytes (CMs). These cells show comparable development to their neonatal counterparts, and in their terminally differentiated state, the individual CMs show action potentials (APs) typical of either atrial, ventricular, or nodal tissues (17, 36). When differentiated, CMs show normal sarcomere formation, have functional cell-cell junctions, beat spontaneously, and express the cardiac isoforms of  $\alpha$ -myosin heavy chain,  $\beta$ -myosin heavy chain, and troponin I (13, 18, 26, 31). The genetic tractability and ease of sampling make ESC-derived CMs an attractive model system in which to study the role of T-type channels. In this study, we characterize the  $I_{\text{Ca,T}}$ , its developmental regulation, and its correlation with mRNA abundance and measures of pacemaker activity.

\*Y. M. Zhang and L. Shang contributed equally to this work.

Address for reprint requests and other correspondence: S. C. Dudley, Jr., Div. of Cardiology, Emory Univ./Atlanta VA Medical Center, 1670 Clairmont Rd., Rm. 111B, Decatur, GA 30033 (E-mail: sdudley@emory.edu).

The costs of publication of this article were defrayed in part by the payment of page charges. The article must therefore be hereby marked "advertisement" in accordance with 18 U.S.C. Section 1734 solely to indicate this fact.

## MATERIALS AND METHODS

*In vitro differentiation of CMs from ESCs.* The R1 mouse ESC line was generously provided by Dr. Kenneth Boheler and was used throughout the study. Undifferentiated ESCs were maintained and expanded on mitotically inactivated fibroblast feeder layers (*passages 2–4*) as described previously (17, 36) using high-glucose DMEM (GIBCO-BRL Life Technologies; Rockville, MD) supplemented with 15% heat-inactivated FBS (selected lots; Life Technologies), L-glutamine (GIBCO-BRL, 200 mM, stock solution diluted 1:100),  $\beta$ -mercaptoethanol (GIBCO-BRL, final concentration  $5 \times 10^{-5}$  M), nonessential amino acids (GIBCO-BRL, 10 mM, stock solution diluted 1:100), and penicillin/streptomycin (GIBCO-BRL, 5,000 U/ml, stock solution diluted 1:5,000). The *in vitro* differentiation of ESCs was initiated by trypsin-EDTA treatment to obtain dissociated single cell suspensions. About 400–800 ESCs were suspended in 20  $\mu$ l of media supplemented with 20% FBS and were placed as hanging drops on the lids of petri dishes filled with PBS. After 2 days, the mass of cells, an embryoid body (EB), was washed from the lid and resuspended for an additional 5 days in fresh media. The 7-day-old EBs were plated onto 0.1% gelatin-coated petri dishes. EBs showed spontaneous beating as early as 2 days after plating. The percentage of EBs with beating areas was recorded at various time points during continued cultivation. To make the measurements, all simultaneously plated EBs were observed. This number was always  $>30$  and usually in the range of 60. The EBs were followed every other day. Beating EBs were defined as those with  $>5\%$  of their area contracting spontaneously. The beating EBs were labeled and followed over time.

*Electrophysiological study on derived CMs.* CMs were isolated at various developmental time points designated as the number of days after plating of the 7-day-old EB. For each time point, spontaneously beating areas of 5–10 EBs were mechanically dissected with a microprobe. The isolated tissue was incubated for 30 min at 37°C with a digestion solution containing (in mM) 120 NaCl, 5.4 KCl, 5  $MgSO_4$ , 5 Na-pyruvate, 20 glucose, 20 taurine, and 10 HEPES (pH 6.9), 1 mg/ml collagenase B (Boehringer Mannheim; Mannheim, Germany), and 30  $\mu$ M  $CaCl_2$  at room temperature. The dissociation process was continued in high- $K^+$  solution for 1 h at room temperature. The high- $K^+$  solution was composed of (in mM) 85 KCl, 30  $K_2HPO_4$ , 5  $MgSO_4$ , 1 EDTA, 2  $Na_2ATP$ , 5 pyruvic acid, 5 creatine, 20 taurine, and 20 glucose, pH 7.4. Single CMs were replated on coverslips coated with 0.1% gelatin and 20  $\mu$ g/ml laminin in cultivation medium and incubated at 37°C. Cells exhibited spontaneous beating after overnight incubation. Electrophysiological studies were carried out 1 to 5 days after the cell isolation.

To measure  $I_{Ca,T}$  immediately before the experiments, culture medium was replaced with a  $Na^+$ -free recording solution consisting of (in mM) 120 *N*-methyl-D-aspartate, 5.4 KCl, 1.8  $CaCl_2$ , 1  $MgCl_2$ , 10 CsCl, 10 tetraethylammonium-Cl, 10 HEPES, and 10 glucose (pH 7.4 by HCl) at 37°C.  $Na^+$ -free conditions have been used to help minimize contamination of the  $Ca^{2+}$  currents by the larger  $Na^+$  current (8, 24). Experiments with tetrodotoxin (TTX), a specific  $Na^+$  channel blocker, confirm the lack of substantial  $Na^+$  current under these conditions. In four experiments, 30  $\mu$ M TTX applied in the perfusion solution did not affect the  $I_{Ca,T}$ , indicating that there was no significant  $Na^+$  current component involved in the recorded current. The peak current was taken as the maximum current observed within 10 ms of the voltage pulse.

To measure spontaneous APs, the culture medium was replaced with a solution consisting of (in mmol/l) 140 NaCl, 5.4 KCl, 1.8  $CaCl_2$ , 1  $MgCl_2$ , 10 HEPES, and 10 glucose (pH 7.4 by NaOH) at 37°C. Thin-wall glass patch pipettes (World Precision Instruments; Sarasota, FL) were pulled to resistance of 2–5 M $\Omega$ . For current measurement, the intracellular solution contained (in mM) 80 KCl, 20 CsCl, 20 tetraethylammonium-Cl, 1  $MgCl_2$ , 3  $MgATP$ , 10 HEPES, and 10 EGTA (pH 7.2 by KOH). For AP measurement, the intracellular solution contained (in mmol/l) 120 KCl, 1  $MgCl_2$ , 3  $MgATP$ , 10 HEPES, and 10 EGTA (pH 7.2 by KOH). Membrane currents and APs were recorded in the whole cell single-electrode voltage-clamp and current-clamp configurations of the patch-clamp technique, respectively, using an Axopatch 200B amplifier and a Digidata 1320 Interface (Axon Instruments; Burlingame, CA). pCLAMP software version 8.0 (Axon Instruments) was used for generation of protocols, data storage, and evaluation.  $Ca^{2+}$  currents were elicited by depolarization of the membrane from the holding potentials to various test potentials and normalized to cell capacitance. Cell capacitance was estimated at the beginning of each experiment. After seal formation, membrane rupture, and equilibration, a single 20-mV hyperpolarization pulse was applied. The resulting capacitive current transient was integrated and divided by the voltage step to determine the cell capacitance. Electronic capacitance compensation was used to minimize current transient during applied pulses. Both measures of capacitance agreed well. Spontaneous APs were recorded, and the rates of slow phase 4 AP depolarization were determined. Data were digitized at 10 kHz and filtered at 2 kHz. Recordings were initiated 5 min after patch break to allow equilibration of the patch pipette solution with the intracellular milieu. After the 5-min equilibration period,  $Ca^{2+}$  currents were stable, suggesting that if L-type  $Ca^{2+}$  current ( $I_{Ca,L}$ ) rundown had occurred, it did so before the recordings.

TTX was dissolved in 50 mM acetic acid to make a stock of 3 mM. Nifedipine stock was made as 10 mM in DMSO, so that the final concentration of DMSO would be  $<0.05\%$  in the perfusing solution.  $Ni^{2+}$  chloride was dissolved in water as a 1 mM stock. All chemicals were purchased from Sigma (St. Louis, MO) unless specified. All data are presented as means  $\pm$  SE. Student's *t*-tests and one-way and two-way ANOVA were employed for statistical analysis.

*Identification of CMs by green fluorescent protein.* A 2.9-kb fragment of the 5' upstream regulatory sequence of the mouse cardiac myosin light chain (MLC)2v gene (GenBank, AF302688) was amplified by PCR and then directly subcloned into pGlow-topo report cloning vector that contained a gene encoding green fluorescent protein (GFP; Invitrogen; Carlsbad, CA). A 659-bp cytomegalovirus (CMV) immediate-early enhancer was amplified by PCR using the pCI-neo mammalian expression vector (Promega; Madison, WI) as the template and primers with *Afl*II and *Kpn*I sites (5' CMV-*Afl*IIU:CTTAAGTCACATGGCTCGACAGATCT; 3' CMV-*Kpn*I/L:GGTACCGGGCGATCGCAGTTGTTACG). This enhancer was subcloned into the GFP vector at an upstream *Afl*II-*Kpn*I location. The final plasmid construct (20  $\mu$ g) was linearized and introduced into  $1-2 \times 10^7$  ESCs with the use of an Eppendorf multipipetator (300 V/100  $\mu$ s). After a 7-day G418 selection, 10 clones were identified by presence of a PCR product spanning the promoter region and GFP exon. Two of the PCR-positive ESC clones were differentiated *in vitro* into EBs. A subset of spontaneously contractile CMs in these EBs showed significant fluorescence at terminal differentiation.

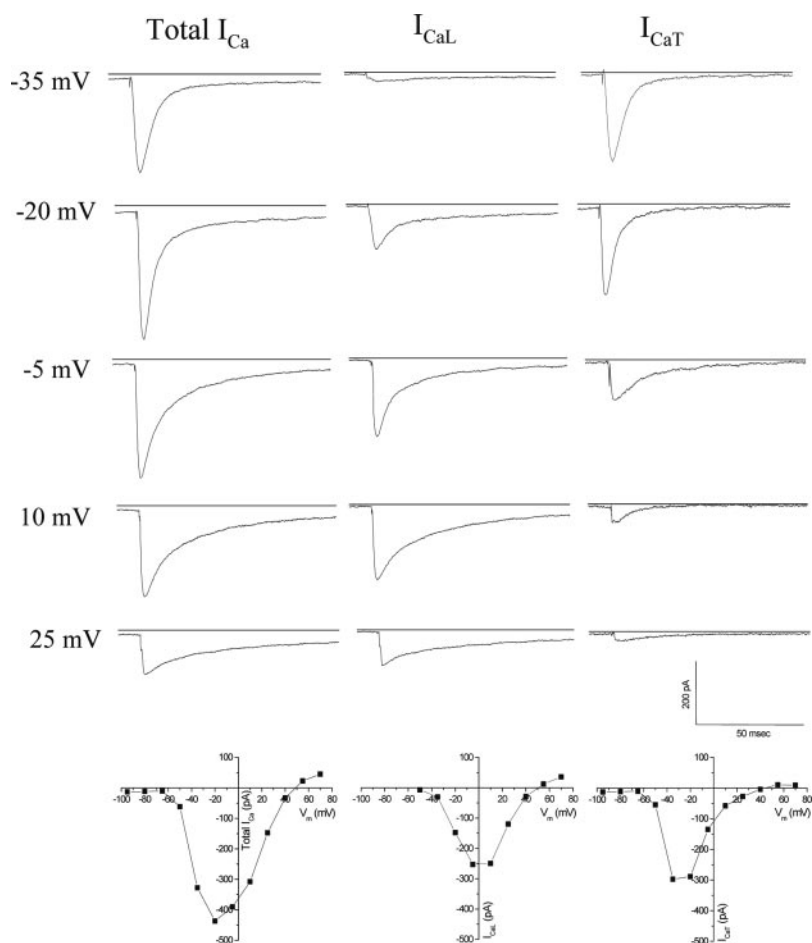


Fig. 1. Comparison of  $Ca^{2+}$  current ( $I_{Ca}$ ), L-type  $I_{Ca}$  ( $I_{Ca,L}$ ), and T-type  $I_{Ca}$  ( $I_{Ca,T}$ ) whole cell currents separated by holding voltage. Whole cell currents were measured in single isolated cardiomyocytes (CMs) 12 days after embryoid body (EB) plating. Total  $I_{Ca}$  and  $I_{Ca,L}$  were measured by using holding potentials  $-90$  and  $-50$  mV, respectively.  $I_{Ca,T}$  was obtained by subtraction of  $I_{Ca,L}$  from total  $I_{Ca}$ . Peak current-voltage curves for  $I_{Ca}$ ,  $I_{Ca,L}$ , and  $I_{Ca,T}$  were plotted at the end of each corresponding column. The horizontal lines indicate the zero current levels.  $V_m$ , membrane potential.

**Analysis of T-channel mRNA abundance from CMs.** EBs at days 4, 10, 16, and 27 after plating were washed with PBS and digested by 0.25% trypsin (GIBCO; Carlsbad, CA), 1 mg/ml collagenase II (Roche Diagnostics; Indianapolis, IN), and 1 ng/ml bovine serum albumin in DMEM medium at  $37^\circ C$  for 10 min. The cells were washed once by DMEM after trituration. Single cells were plated at  $1 \times 10^4$  cells/plate on microscope slides. After 2 h, the attached cells were washed with PBS, then immediately fixed in 95% ethanol for 3–5 min, and then rinsed in water and dehydrated progressively in 70%, 95%, and 100% ethanol for 30 s each. Finally, the cells were treated with xylenes for 5 min. The fluorescent cells were picked with the use of a laser capture microdissection system (Arcturus; Mountain View, CA)  $<2$  h after fixation to avoid RNA degradation.

At each time point, total RNA from 50 GFP-expressing cells was isolated using the PicoPure RNA isolation kit (Arcturus) in a total volume of 24  $\mu$ l according to the manufacturer's protocol. Reverse transcription was carried out for 60 min at  $37^\circ C$  in a final volume of 40  $\mu$ l containing 24  $\mu$ l of RNA, 40  $\mu$ M oligo(dT), 20 units of RNase inhibitor, and 2  $\mu$ l of Sensiscript Reverse Transcriptase (Stratagene; La Jolla, CA). The enzyme was inactivated by heating the reaction mixture to  $93^\circ C$  for 5 min, followed by rapid cooling on ice. Quantitative real-time PCR was performed using the iCycler IQ Multi-Color Real-Time Detection System (Bio-Rad Laboratories; Hercules, CA) and software. Taqman probe was labeled with a 5' reporter (FAM) and a 3' quencher dye (BHQ1). The  $Ca_v3.1$  forward and reverse primers were designed based on the reported sequence (GenBank accession

no. NM\_009783). For each experimental sample, the amount of target gene was determined from an absolute standard curve established with fivefold serial dilution of  $Ca_v3.1$  cRNA. To make this cRNA, a 157-bp segment from  $Ca_v3.1$  cDNA was amplified by PCR and cloned into the pCRII-topo cloning vector (Invitrogen) and then confirmed by restriction enzyme digestion and sequencing. This plasmid was used as a template for transcription of cRNA with the use of the mCAP mRNA Capping Kit (Stratagene). The experiments were run in duplicate. PCR was performed with Taqman Universal PCR Master mix (Applied Biosystems; Foster City, CA) using 8  $\mu$ l of cDNA, 250 nM of probe (5'-FAM-CCTTCGTGCTGACGGCCAGT-BHQ1-3'), 300 nM primers ( $Ca_v3.1F$ : 5'-ACCTGCTACAACACCGTCATCTCAC-3',  $Ca_v3.1R$ : 5'-TCCAGCTCCGCTCCAACCTC-3') in a 50- $\mu$ l final reaction mixture. The AmpliTaq Gold Enzyme was activated for 10 min at  $95^\circ C$ . Each of the 50 PCR cycles consisted of 15-s denaturation at  $95^\circ C$  and hybridization of primers and probe for 1 min at  $60^\circ C$ .

**Immunostaining of EBs from in vitro differentiated ESCs.** Technical details have been described previously (3). Briefly, anti- $Ca_v3.1$  antibodies (2xG1, 2xH1) were prepared against peptides derived from the  $Ca_v3.1$  and  $Ca_v3.2$  T-type channel sequences (2xG1: FVCQGEDTRNITNKSDCAEAS; 2xH1: YYCEGPDTRNISTKAQCRAAH) and were immunoaffinity purified (Bethyl Laboratories; Montgomery, TX). Antibodies were also immunoabsorbed to "DTRNI" peptide to eliminate potential cross reactivity because of that common epitope. The EBs from ESCs were fixed in 4% paraformaldehyde/PBS before being mounted in embedding compound for cryosec-

tioning. Cryosections (12  $\mu\text{m}$ ) were blocked with 1% normal goat serum-PBS and then incubated with preimmune serum (negative control) or primary antibody (diluted in PBS/0.1% Triton X-100) for 1 h. Immunodetection was accomplished with ABC Elite reagents using the VIP substrate kit as the chromogenic substrate (Vector Laboratories; Burlingame, CA).

## RESULTS

**Electrophysiological characterization of  $I_{\text{Ca,T}}$  in ESC-derived CMs.** The  $I_{\text{Ca,T}}$  was identified using two different classic methodologies (11, 24) that gave comparable results. In the first method, total and  $I_{\text{Ca,L}}$  were elicited by depolarizing voltage steps from holding potentials of  $-90$  and  $-50$  mV, respectively. At  $-50$  mV, the cardiac  $I_{\text{Ca,T}}$  is completely inactivated, and  $I_{\text{Ca,T}}$  was calculated as the net current remaining after subtraction of the remaining L-type from the total  $\text{Ca}^{2+}$  current recorded at  $-90$  mV. Figure 1 shows a family of membrane currents and derived peak current-voltage relationship ( $I$ - $V$ ) curves from a representative ESC-derived CM.  $I_{\text{Ca,T}}$  activated at voltages near  $-60$  mV, peaked at about  $-30$  mV and reversed near  $40$  mV. In CMs, the amplitude of  $I_{\text{Ca,T}}$  and  $I_{\text{Ca,L}}$  was in the same range.

The second method was to separate  $I_{\text{Ca,L}}$  and  $I_{\text{Ca,T}}$  pharmacologically. Because there is no completely specific T-type channel blocker, we used the L-type channel blocker nifedipine to eliminate the  $I_{\text{Ca,L}}$ . The total  $\text{Ca}^{2+}$  current was measured using a holding potential of  $-90$  mV, and then  $30$   $\mu\text{M}$  nifedipine was added in the perfusion solution to eliminate the L-type current. The current remaining was taken as  $I_{\text{Ca,T}}$ . The results obtained were comparable between the two methods (Fig. 2).

**Pharmacological identification of the T-type channel isoform in ESC-derived CMs.** We attempted to identify the isoform responsible for the  $I_{\text{Ca,T}}$  in ESC-derived CMs. It has been suggested that  $\text{Ca}_v3.1$  and  $\text{Ca}_v3.2$  are expressed in mammalian heart (2, 35) but only  $\text{Ca}_v3.1$  is expressed in the embryonic mouse heart (3). Because  $\text{Ca}_v3.1$  is more resistant to  $\text{Ni}^{2+}$  than  $\text{Ca}_v3.2$  (15), we tested the  $\text{Ni}^{2+}$  sensitivity of the T-type channel. The addition of  $5$   $\mu\text{M}$   $\text{Ni}^{2+}$  in the perfusion solution resulted in a slight but not significant decrease in  $I_{\text{Ca,T}}$ , where 91% of control current remained ( $n = 5$ ). Nevertheless,  $100$   $\mu\text{M}$   $\text{Ni}^{2+}$  completely blocked  $I_{\text{Ca,T}}$  ( $n = 5$ ), suggesting the more  $\text{Ni}^{2+}$ -resistant  $\text{Ca}_v3.1$  was responsible for the  $I_{\text{Ca,T}}$  currents shown in Fig. 2. Immunohistochemical analysis confirmed the presence of  $\text{Ca}_v3.1$  in derived CMs, consistent with our electrophysiological identification (Fig. 3), and there was no evidence for  $\text{Ca}_v3.2$  expression in EBs (data not shown).

**T-type current regulation during development of derived CMs.** To evaluate the developmental regulation of the T-type channel, we characterized current changes in our in vitro CM differentiation system. Peak  $I$ - $V$  relationships were obtained at different stages of differentiation (Fig. 4, A and B). The amplitude of  $I_{\text{Ca,T}}$  changed in a biphasic manner with time in culture. At days 4, 7, 14, and 19 after EB plating, using

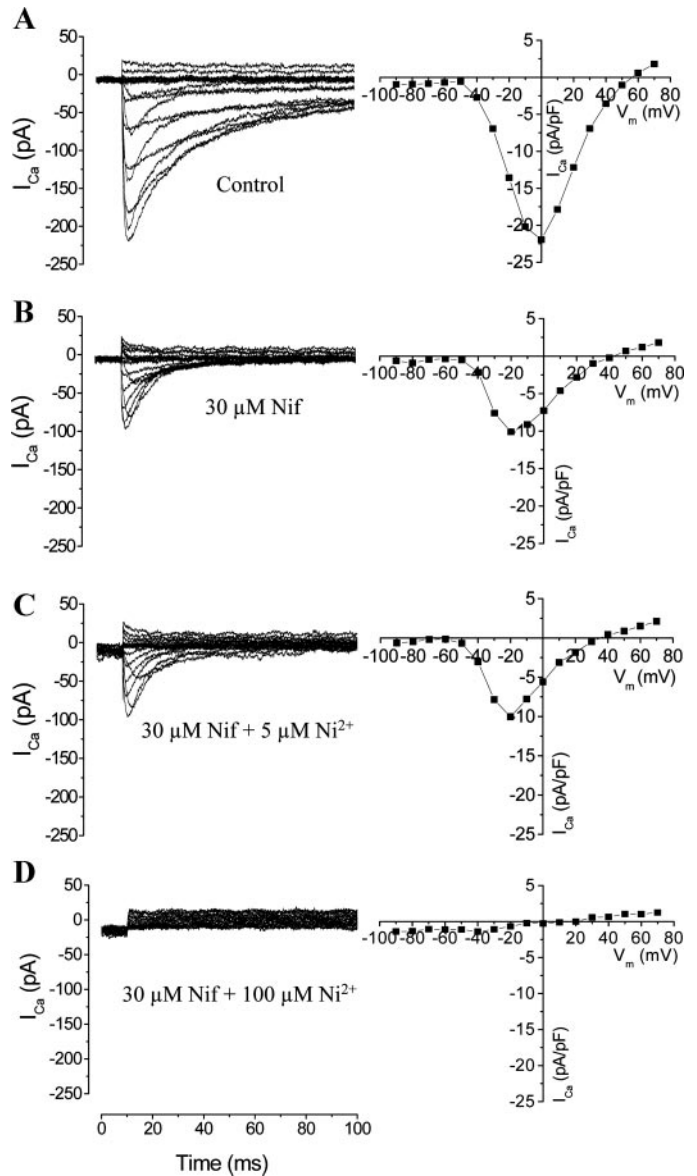


Fig. 2.  $I_{\text{Ca,T}}$  from embryonic stem cell (ESC)-derived CMs are resistant to  $5$   $\mu\text{M}$   $\text{Ni}^{2+}$ . Whole cell currents were measured in single isolated CMs 7 days after EB plating. Total  $\text{Ca}^{2+}$  currents were obtained under control conditions (A) and in the presence of  $I_{\text{Ca,L}}$  channel blocker nifedipine ( $30$   $\mu\text{M}$  Nif) (B). The current remaining after  $I_{\text{Ca,L}}$  channel blockade showed little sensitivity to a low concentration of  $\text{Ni}^{2+}$  ( $5$   $\mu\text{M}$ ) (C), but a high concentration of  $\text{Ni}^{2+}$  ( $100$   $\mu\text{M}$ ; D) completely blocked the current, suggesting that the  $\text{Ca}_v3.1$  gene product is likely responsible for most  $I_{\text{Ca,T}}$  in these cells.

the subtraction method by holding the membrane potential at  $-90$  and  $-50$  mV, respectively, the peak  $I_{\text{Ca,T}}$  (pA/pF) was  $-5.3 \pm 0.8$  ( $n = 7$ ),  $-8.1 \pm 1.9$  ( $n = 6$ ),  $-11.4 \pm 1.9$  ( $n = 7$ ), and  $-5.0 \pm 1.1$  ( $n = 7$ ), respectively ( $P = 0.02$ , one-way ANOVA). Comparison of individual means showed significant differences when comparing days 4 and 14 and days 14 and 19 ( $P < 0.05$ ,  $t$ -test). A similar pattern of upregulation in early development was observed by the second technique to isolate  $I_{\text{Ca,T}}$ . By applying nifedipine to block  $I_{\text{Ca,L}}$ , we obtained  $I_{\text{Ca,T}}$  (pA/pF) of  $-5.6 \pm 1.5$  ( $n = 4$ ) and

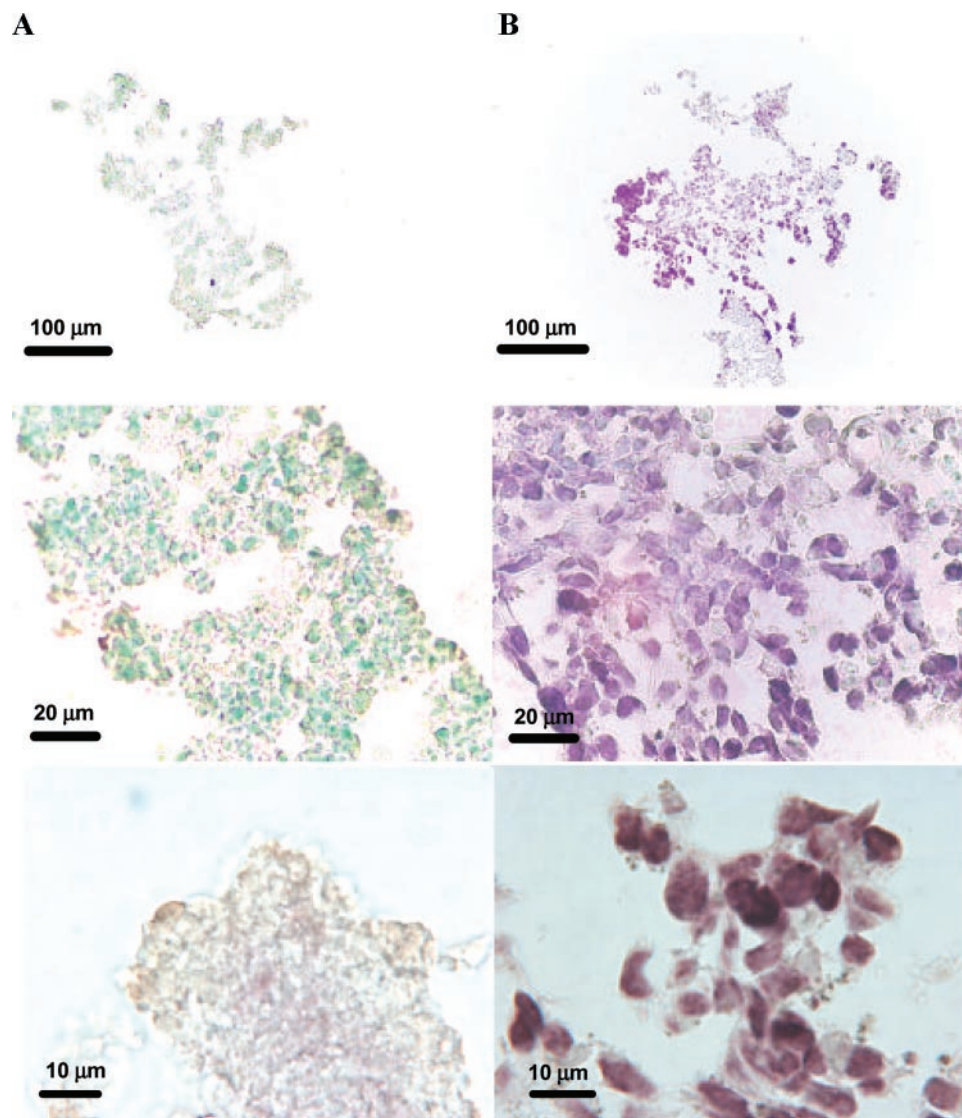


Fig. 3. Immunohistochemical staining for the presence of  $Ca_v3.1$ . *A*: dissected, beating areas of EBs in the absence of anti- $Ca_v3.1$  antibody (magnifications  $\times 100$ ,  $\times 400$ , and  $\times 1,000$ ). *B*: corresponding views after antibody staining. Significant staining only supports the idea that  $Ca_v3.1$  underlies  $I_{Ca,T}$  in these cells.

$-11.2 \pm 1.6$  ( $n = 6$ ) at 7+3–5 and 7+9–15 days after EB plating, respectively. The data were not statistically significantly different from the data obtained by the subtraction method.

$I_{Ca,L}$  showed a similar pattern but the change in peak current over time was less pronounced and was not statistically significant. Peak  $I_{Ca,L}$  was  $-7.9 \pm 1.3$  ( $n = 7$ ),  $-12.0 \pm 2.7$  ( $n = 6$ ),  $-10.6 \pm 3.0$  ( $n = 6$ ), and  $-8.2 \pm 1.2$  ( $n = 5$ ), respectively ( $P = 0.51$ , one-way ANOVA). There were no statistically significant differences in these means as determined by Student's *t*-tests.

**Correlation of T-type channel current to mRNA abundance in CMs.** To investigate the mechanism of control of  $I_{Ca,T}$ , we established a transgenic construct that expressed GFP under control of the ventricular-specific MLC2v and CMV promoters. When the pCMV-2.9MLC2v-GFP stable ESC clone was differentiated,  $\sim 5$ –10% of the cells of the EB demonstrated strong GFP expression. Fluorescence was detected as early as day 2 after EB plating, and the number of cells ex-

pressing GFP increased at later stages. Approximately 80% of contractile cells within the beating areas of EBs showed labeling, suggesting some inhomogeneity within these cell aggregates.

RT-PCR using total RNA isolated from EBs showed that the  $Ca_v3.1$  transcript was present in cells at day 7+0. To correlate  $Ca_v3.1$  mRNA abundance and  $I_{Ca,T}$ , CMs expressing GFP were fixed and selected by laser capture microdissection. For each developmental time point, 30–50 EBs were used for cell isolation, and  $\sim 1 \times 10^4$  cells were scanned for capture. RT-PCR suggested developmental regulation of  $Ca_v3.1$  message (Fig. 4C). These changes were analyzed further by quantitative real-time RT-PCR. Because no genes have been established as an internal reference during heart development, total RNA was isolated from these cells, analyzed by real time PCR, and compared with an absolute standard. The real-time RT-PCR results showed that  $Ca_v3.1$  mRNA copy number was low at day 4 (2 copies/cell), increased significantly by day 10 (27 copies/cell;  $P < 0.01$ ),

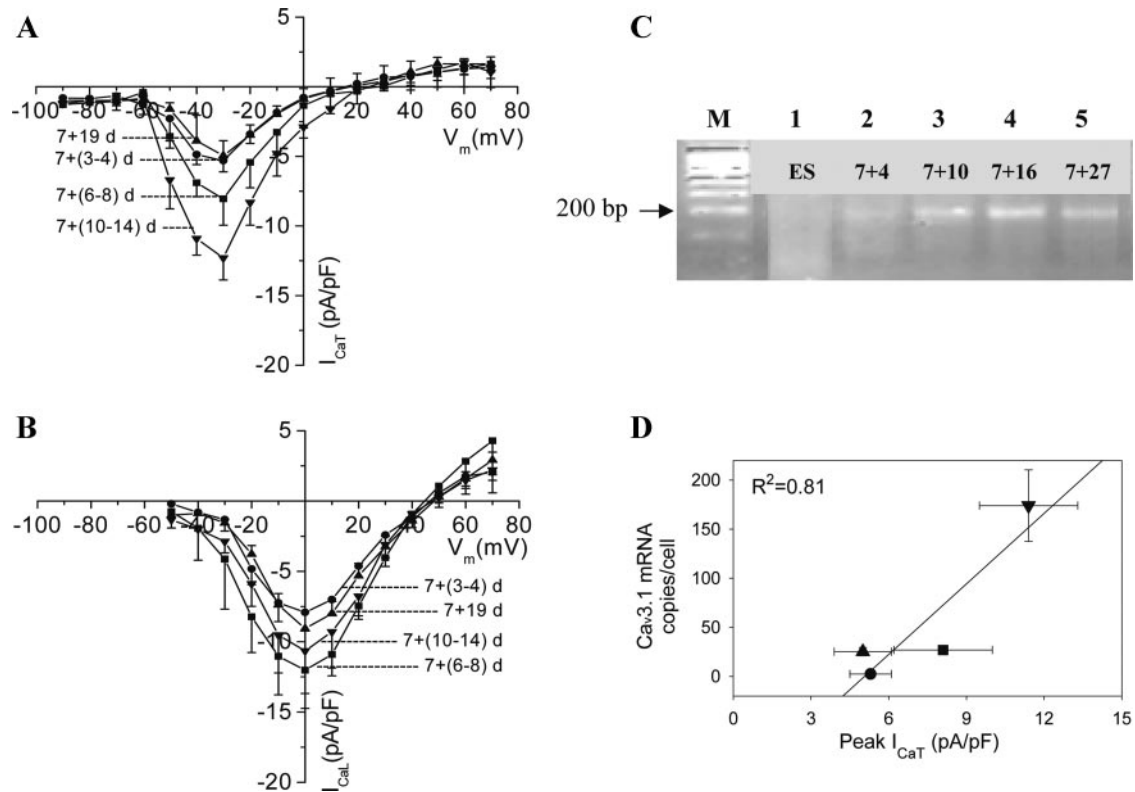


Fig. 4. Developmental regulation of murine  $I_{Ca,T}$  and  $Ca_v3.1$  mRNA abundance. Peak current-voltage curves of  $I_{Ca,T}$  (A) and  $I_{Ca,L}$  (B) are shown as a function of developmental time in ESC-derived CMs. Whole cell currents were measured in single isolated CMs at varied days after EB plating. Total  $I_{Ca}$  and  $I_{Ca,T}$  were measured by using holding potentials  $-90$  and  $-50$  mV, respectively.  $I_{Ca,T}$  was obtained from subtraction of  $I_{Ca,L}$  from total  $I_{Ca}$ .  $I_{Ca,T}$  showed more prominent regulation with time than  $I_{Ca,L}$ . ●, 7+(3–4) days; ■, 7+(6–8) days; ▼, 7+(10–14) days; and ▲, 7+19 days. C and D show mRNA abundance in GFP-labeled CMs derived from in vitro differentiated ESCs correlates with the peak  $I_{Ca,T}$ . RNA was isolated from 50 labeled CMs by laser capture microdissection. A 157 bp  $Ca_v3.1$  RT-PCR product was subjected to 1.2% agarose gel electrophoresis and ethidium bromide staining. C: RT-PCR results demonstrated that  $Ca_v3.1$  mRNA copy number was low at day 4 (lane 2), increased significantly by day 10 (lane 3), peaked at day 16 (lane 4), and declined significantly at day 27 (lane 5).  $Ca_v3.1$  mRNA was not detectable in undifferentiated ESCs (lane 1). Lane M shows a 100-bp molecular weight marker. The arrow indicates the 200-bp fragment. D: changes in peak  $I_{Ca,T}$  correlated with changes in  $Ca_v3.1$  mRNA abundance ( $r^2 = 0.81$ ). ●, 7+(4–6) days; ■, 7+(7–11) days; ▼, 7+(12–16) days; and ▲, 7+(19–27) days.

peaked at day 16 (174 copies/cell;  $P = 0.04$  compared with day 10), and declined significantly at day 27 (25 copies/cell;  $P = 0.04$  compared with day 16). The mRNA abundance correlated strongly with peak T-type channel current amplitude obtained at 7+4–6 days, 7+7–11 days, 7+12–16 days, and 7+19–27 days (Fig. 4D;  $r^2 = 0.81$ ). This suggested that developmental changes in T-type channel current amplitude in these cells might be controlled at the level of mRNA abundance.

**Correlation of T-type channel current to measures of pacemaker activity in CMs.** Because  $I_{Ca,T}$  has been implicated in pacemaker function, we studied the relationship between the percentage of EBs containing beating areas (34), an approximation of pacemaker function, and the amount of  $I_{Ca,T}$ . The percentage of the beating areas in each EB was followed during developmental stages. The percentage of beating areas of EBs showed a biphasic behavior, rising and falling over the same time period as T-type channel expression (34). At 7+4–6, 7+7–11, 7+12–16, and 7+19–27

days after plating, the percentage of beating EBs were  $30.0 \pm 9.5$ ,  $51.6 \pm 12.7$ ,  $54.6 \pm 9.8$ , and  $26.7 \pm 6.9$  ( $P < 0.05$ ; one-way ANOVA). The expression of T-type current and the percentage of EBs with beating areas were highly correlated ( $r^2 = 0.86$ ; Fig. 5A).

At the single cell level, we studied spontaneous automatic activity and its correlation with  $I_{Ca,T}$  levels during development. The spontaneous beating frequencies showed the tendency to increase with the maturity of differentiation and decrease when the cells were terminally differentiated (Fig. 6). The frequencies of APs were (in Hz) the following:  $0.76 \pm 0.15$  ( $n = 6$ ),  $1.00 \pm 0.12$  ( $n = 5$ ),  $1.26 \pm 0.24$  ( $n = 10$ ),  $0.42 \pm 0.14$  ( $n = 4$ ) at 7+4–6, 7+7–11, 7+12–16, and 7+19–27 days. The phenomenon was consistent with the percentage of EBs with beating areas, and the spontaneous beating frequency correlated with the T-type current ( $r^2 = 0.81$ ; Fig. 5B).

$I_{Ca,T}$  has been implicated in pacemaker function by virtue of the fact that it should be active during the voltage range involved in phase 4 depolarization. We

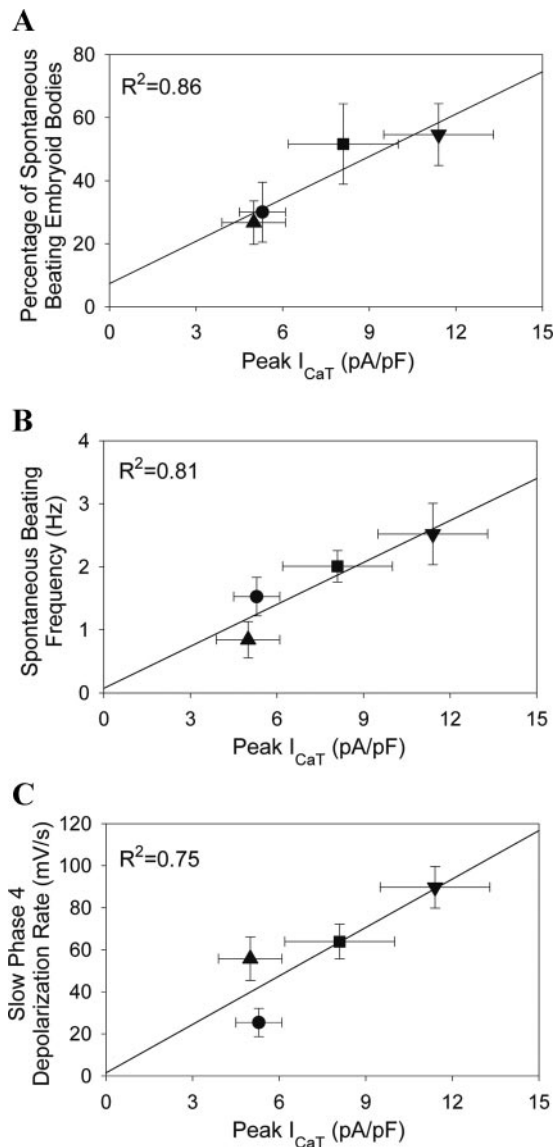


Fig. 5. Relationship between peak  $I_{Ca,T}$  and measures of pacemaker activity, including the percentage of EBs with beating areas (A), spontaneous single cell beating frequency (B), and slow phase 4 depolarization rate (C). During development, changes in peak  $I_{Ca,T}$  correlated with the temporal variation in the percentage of beating EBs ( $r^2 = 0.86$ ), changes in peak  $I_{Ca,T}$  correlated with changes in spontaneous beating frequency of single cells ( $r^2 = 0.81$ ), and changes in peak  $I_{Ca,T}$  correlated with slow phase 4 depolarization rate ( $r^2 = 0.75$ ). The data were expressed as means  $\pm$  SE.  $\bullet$ , 7+(4–6) days;  $\blacksquare$ , 7+(7–11) days;  $\blacktriangledown$ , 7+(12–16) days; and  $\blacktriangle$ , 7+(19–27) days.

attempted to correlate the phase 4 depolarization rates in spontaneous beating cells with the amount of T-type current present. Phase 4 depolarization typically had fast and slow components. The slow depolarization rates (mV/s) were  $25.4 \pm 6.7$  ( $n = 5$ ) at 7+4–6 days, increased to  $63.9 \pm 8.2$  ( $n = 6$ ) at 7+7–11 days, and to  $89.7 \pm 9.9$  ( $n = 14$ ) at 7+12–16 days, and decreased to  $55.7 \pm 10.4$  ( $n = 4$ ) at 7+19–27 days ( $P < 0.05$ , one-way ANOVA). The fast depolarization rates (mV/s) were  $55.9 \pm 9.0$  ( $n = 5$ ) at 7+4–6 days, increased to  $119.1 \pm 8.4$  ( $n = 6$ ) at 7+7–11 days, and to  $158.2 \pm 11.2$  ( $n = 14$ ) at 7+12–16 days, and decreased to

$108.8 \pm 12.6$  ( $n = 4$ ) at 7+19–27 days ( $P < 0.05$ , one-way ANOVA). At later differentiation stages, cells tended to cease their spontaneous activity, so it was not technically feasible to measure phase 4 depolarization rates. Nevertheless, for spontaneous beating cells, both slow and fast phase 4 depolarization rates correlated with the  $I_{Ca,T}$  ( $r^2 = 0.75$  for slow phase, and  $r^2 = 0.70$  for fast phase). The correlation of the slow phase with  $I_{Ca,T}$  during development is shown in Fig. 5C. In addition, T-type channels were active at the voltage range involved in phase 4 depolarization. Slow phase 4 depolarization occurred in a range of membrane potentials from  $-62$  to  $-50$  mV. This range is consistent with the activation range of the  $I_{Ca,T}$ , making it reasonable to consider the possibility of the  $I_{Ca,T}$  having a physiological role in pacemaking. Despite these observations,  $Ni^{2+}$  had a variable effect on automatic activity of EBs, ranging from reduced rates to abolishment of activity. The origin of the variability was unclear.

## DISCUSSION

In the present study, we demonstrated that  $I_{Ca,T}$  was regulated during development in mouse ESC-derived CMs, the  $Ca_v3.1$  gene encoded the  $I_{Ca,T}$  in these cells, the T-type current changes correlated with mRNA abundance, and  $I_{Ca,T}$  correlated with multicellular and isolated cell measures of pacemaker activity.

*Ca<sub>v</sub>3.1 encoded T-type channel current in ESC-derived CMs.* Electrophysiology, pharmacology, immunohistochemistry, and molecular biology lines of evidence support the conclusion that the T-type channel in ESC-derived CMs results from  $Ca_v3.1$  gene expression. The  $I_{Ca,T}$  we observed had similar properties to the current in other systems. Our  $I_{Ca,T}$  showed activation at about  $-60$  mV, peaked at about  $-30$  mV with an apparent reversal potential of  $\sim 40$  mV, which was similar to  $Ca^{2+}$  currents recorded in previous studies in canine cardiac Purkinje cells (6, 7) and recent studies in rat cardiac cells (16, 23), although Pignier and Potreau (24) had observed a more right-shifted nifedipine-resistant  $Ca^{2+}$  current  $I-V$  curve. Also, the  $I-V$  curves are consistent with a study in human embryonic kidney HEK-293 cells expressing the  $Ca_v3.1$  channel (29). The T-type channel in CMs was relatively resistant to  $Ni^{2+}$  block, another characteristic of  $Ca_v3.1$  (15). Immunohistochemistry supported the presence of  $Ca_v3.1$  and not  $Ca_v3.2$ . Finally,  $Ca_v3.1$  mRNA abundance correlated well with the amount of T-type channel current.

We observed some variation in the peak of  $I_{Ca,T}$  with development, shifting to more hyperpolarized potentials at later developmental stages. A similar shift has been reported in the chick ventricle. In Fig. 2, the cells were studied 7 days after plating and peaked at about  $-20$  mV. On the other hand,  $I_{Ca,T}$  peaked at about  $-30$  mV in Fig. 1, in which the cell was studied 12 days after plating. Kawano and DeHaan (11) reported that the half-activation potential of  $I_{Ca,T}$  was  $-29$  mV in 7-day embryonic chick cells and  $-38$  mV in 14-day cells.

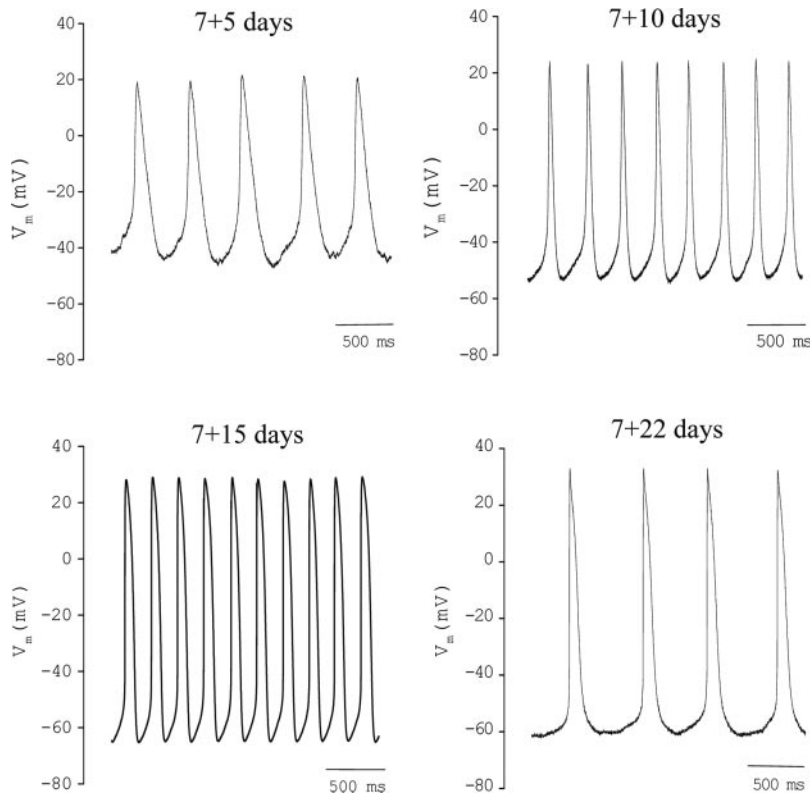


Fig. 6. Sample recordings of automatic activity in ESC-derived cardiomyocytes. Action potentials in CMs at 7+5 days, 7+10 days, 7+15 days, and 7+22 days. ESC-derived cardiomyocytes with spontaneous beating activity were studied in the current clamp mode at 37°C.

*T*-type channel current was developmentally regulated. We observed a biphasic change in T-type channel current during CM differentiation that was similar to that seen in mouse cardiac development (3). The  $I_{Ca,T}$  variation during differentiation is consistent with studies in postnatal rat myocytes (16, 32), and a similar pattern of downregulation has been seen in development of both atrial and ventricular myocytes, providing another line of evidence that CM development in vitro is similar to myocyte development in situ (11, 16).

We separated  $I_{Ca,T}$  from  $I_{Ca,L}$  by two classic methods, pharmacological block of the  $I_{Ca,L}$  and physiological separation by holding voltage. The resulting current that we defined as  $I_{Ca,T}$  showed the expected characteristics such as high-voltage activation and  $Ni^{2+}$  sensitivity. Moreover, the tight correlation of this current to  $Ca_v3.1$  mRNA abundance suggests that it is unlikely that there was substantial contribution by other channels to our  $I_{Ca,T}$ . Although we did not study total protein levels with Western blotting or other techniques, this correlation diminishes the likelihood of substantial channel trafficking or posttranslational modification/regulation as the main mechanisms of  $I_{Ca,T}$  variations with development.

It was our intention to study the role of T-type currents in ESC development to CMs. The strong correlation of  $I_{Ca,T}$  and  $Ca_v3.1$  mRNA abundance was made by measuring currents in spontaneously active, ESC-derived CMs and comparing that to mRNA levels from GFP positive cells, presumably destined for the ventricular lineage. The strong correlation of current to mRNA despite a more heterogeneous population

studied electrophysiologically suggests that the correlation may be even more robust in ventricular cells than we report here, because ~80% of derived CMs ultimately show a ventricular-like AP morphology. Nevertheless, it is possible that the change in T-type channel current and correlation of  $I_{Ca,T}$  and mRNA abundance are ventricular specific, and this experimental design may explain in part why the relationship of  $I_{Ca,T}$  and  $Ca_v3.1$  mRNA abundance does not pass through the origin.

Our study revealed that  $I_{Ca,T}$  in derived CMs was similar to the amount of L-type current. The density of  $I_{Ca,T}$  in ESC-derived CMs was similar to the  $I_{Ca,T}$  measured in embryonic chick cardiac cells (11). In chick cells,  $I_{Ca,T}$  was larger than  $I_{Ca,L}$ , however. Consistent with our observations, Leuranguer et al. (16) recently reported similar levels of  $I_{Ca,T}$  and  $I_{Ca,L}$  in early postnatal period in rat atrial myocytes. In ESC-derived CMs, we observed that  $I_{Ca,T}$  was about sevenfold larger than  $I_{Ca,T}$  reported by Xu and Best (33) (~1.5 pA/pF) and about twofold higher than  $I_{Ca,T}$  reported by Leuranguer et al. (~6 pA/pF). These differences might be related to the spontaneous contractile properties of our derived CMs because Zhou and Lipsius (37) have found that  $I_{Ca,T}$  is about fivefold higher in latent atrial pacemaker cells than in nonpacemaker atrial myocytes. Also, the current amplitude might depend on the developmental stage (i.e., embryo vs. postnatal) (11, 16, 32).

These variations in the relative amounts of the T- and L-type currents may be the result of differences in experimental conditions. All of our measurements

were made under uniform  $Na^+$ -free conditions 5 min after cell membrane rupture. Any  $Ca^{2+}$  loading or L-type  $Ca^{2+}$  channel rundown under these conditions should be constant and, therefore, not invalidate the findings of developmental  $I_{Ca,T}$  regulation. Nevertheless, they could have affected the L-to-T-type current ratio. Any effects are likely to be larger on the L-type current because Huang et al. (8) have recently reported that the T-type current is similar with or without extracellular  $Na^+$ . These effects notwithstanding, the high level of T-type current and the prominent developmental regulation imply a potentially important physiological role for this channel.

*Implications for the possible physiological roles of the T-type channel.* The physiological roles of the  $I_{Ca,T}$  are not clear. In our study, the current density was correlated with the percentage of EBs showing spontaneously beating areas, with single cell beating frequency, and with the rate of phase 4 depolarizations in spontaneously active cells. These suggest that  $I_{Ca,T}$  probably plays a role in the spontaneous contractile activity in developing heart, possibly linking rhythmic contraction to myocyte development (10). The role of the channel in pacemaking activity is supported by a study of Hagiwara et al. (5). In rabbit sinoatrial node cells, blockade of  $I_{Ca,T}$  by 40  $\mu M$   $Ni^{2+}$  induced bradycardia not attributable to the pacemaker current or the  $K^+$  current. Also, experiments from sinoatrial and atrial pacemakers have led to the conclusion that  $I_{Ca,T}$  window current contributes to pacemaker activity primarily during the late phase of the pacemaker potential (5, 9). While  $I_{Ca,T}$  regulation paralleled pacemaker activity, suggesting a role for  $I_{Ca,T}$  in pacemaking, our experiments with  $Ni^{2+}$  added to EBs, where the response ranged from reduced rates to abolishment of automatic activity, and evidence of pacemaker activity in a  $Ca_v3.1$  T-type  $Ca^{2+}$  channel knockout mouse recently reported by Kim et al. (12) does not support an absolute requirement for  $I_{Ca,T}$  in pacemaking.  $I_{Ca,T}$  could possibly be part of the pacemaking apparatus, but redundant pacemaker mechanisms have been developed to support this critical physiological need.

Possibly,  $I_{Ca,T}$  is important in early excitation-contraction coupling in cardiomyocytes. During early differentiation (7+5–8 days) nifedipine did not block spontaneous contractions observed under the light microscope ( $n = 4$ ). This observation is consistent with the experiments of Viatchenko-Karpinski et al. (30), suggesting that the L-type channel may not play the same role in excitation-contraction coupling as it does in mature CMs. It is possible that the T-type channel, with its significant expression during embryonic development, might play an important role in the spontaneous contraction in early cardiac development, although upregulation of an alternative L-type channel with low affinity for dihydropyridines has been proposed to explain similar observations in a  $Ca_v1.2$  knockout mouse (27).

Interestingly, increased  $I_{Ca,T}$  has been observed under pathological conditions, such as in hypertrophied cardiac cells (4, 19) and in failing myocardium (28),

suggesting that upregulation of the T-type current may be part of reversion to the fetal gene program. The expression of the T-type channel might contribute to aberrant rhythmic activity seen with these conditions. Recently, we have observed that ESC-derived CMs have relatively long AP durations compared with adult mouse cardiac cells (36) and that ESC-derived CMs show enhanced proclivity for triggered activity. Some of these properties might be the result of the relatively large T-type channel currents found in these cells. For example, the correlation of phase 4 slow depolarizing rate and the  $I_{Ca,T}$  amplitude suggests that  $I_{Ca,T}$  might play a role in the initiation of delayed after-depolarizations.

Alternatively, T-type channels may play a role in CM proliferation. T-type channels have been related to cell growth (33) and myoblast fusion (1). Notably, a  $Ca_v3.1$  T-type channel knockout mouse reportedly had normal heart differentiation as determined by histology (12). While this suggests that this T-type channel is not essential for cardiac development, full evaluation of the phenotype and the role of compensatory regulation of other  $Ca^{2+}$  channels have not been explored.

In summary, in vitro differentiated CMs express  $Ca_v3.1$ . The expression of this channel is developmentally regulated, predominately at the level of mRNA abundance. This regulation is similar to that seen with in situ differentiating CMs, providing another line of evidence that the in vitro system is a reasonable model in which to study cardiac cellular differentiation. The correlation of this current with measures of pacemaker activity suggests that T-type channels have an important role in this function, although the knockout mouse suggests that the role may be as a facilitator rather than a requirement.

## DISCLOSURES

This work was supported by a Scientist Development Award from the American Heart Association, a Grant-In-Aid from Southeast Affiliate of American Heart Association, a Veterans Affairs Merit Review Award, a Procter and Gamble University Research Exploratory Award, National Heart, Lung, and Blood Institute Grant HL-64828 (all to S. C. Dudley), National Institute of General Medical Sciences Grant GM-60448 (to C. Hartzell), and National Research Service Award Institutional Training Grant HL-07745 (to Y. M. Zhang).

## REFERENCES

1. Bijlenga P, Liu JH, Espinos E, Haenggeli CA, Fischer-Lougheed J, Bader CR, and Bernheim L. T-type  $\alpha 1H$   $Ca^{2+}$  channels are involved in  $Ca^{2+}$  signaling during terminal differentiation (fusion) of human myoblasts. *Proc Natl Acad Sci USA* 97: 7627–7632, 2000.
2. Cribbs LL, Lee JH, Yang J, Satin J, Zhang Y, Daud A, Barclay J, Williamson MP, Fox M, Rees M, and Perez-Reyes E. Cloning and characterization of  $\alpha 1H$  from human heart, a member of the T-type  $Ca^{2+}$  channel gene family. *Circ Res* 83: 103–109, 1998.
3. Cribbs LL, Martin BL, Schroder EA, Keller BB, Delisle BP, and Satin J. Identification of the T-type calcium channel ( $Ca_v3.1d$ ) in developing mouse heart. *Circ Res* 88: 403–407, 2001.
4. Furukawa T, Ito H, Nitta J, Tsujino M, Adachi S, Hiroe M, Marumo F, Sawanobori T, and Hiraoka M. Endothelin-1 enhances calcium entry through T-type calcium channels in

- cultured neonatal rat ventricular myocytes. *Circ Res* 71: 1242–1253, 1992.
5. **Hagiwara N, Irisawa H, and Kameyama M.** Contribution of two types of calcium currents to the pacemaker potentials of rabbit sino-atrial node cells. *J Physiol* 395: 233–253, 1988.
  6. **Hirano Y, Fozzard HA, and January CT.** Characteristics of L- and T-type  $Ca^{2+}$  currents in canine cardiac Purkinje cells. *Am J Physiol Heart Circ Physiol* 256: H1478–H1492, 1989.
  7. **Hirano Y, Fozzard HA, and January CT.** Inactivation properties of T-type calcium current in canine cardiac Purkinje cells. *Biophys J* 56: 1007–1016, 1989.
  8. **Huang B, Qin D, Deng L, Boutjdir M, and Sherif N.** Reexpression of T-type  $Ca^{2+}$  channel gene and current in post-infarction remodeled rat left ventricle. *Cardiovasc Res* 46: 442–449, 2000.
  9. **Huser J, Blatter LA, and Lipsius SL.** Intracellular  $Ca^{2+}$  release contributes to automaticity in cat atrial pacemaker cells. *J Physiol* 524: 415–422, 2000.
  10. **Irisawa H, Brown HF, and Giles W.** Cardiac pacemaking in the sinoatrial node. *Physiol Rev* 73: 197–227, 1993.
  11. **Kawano S and DeHaan RL.** Developmental changes in the calcium currents in embryonic chick ventricular myocytes. *J Membr Biol* 120: 17–28, 1991.
  12. **Kim D, Song I, Keum S, Lee T, Jeong MJ, Kim SS, McEnery MW, and Shin HS.** Lack of the burst firing of thalamocortical relay neurons and resistance to absence seizures in mice lacking  $\alpha 1G$  T-type  $Ca^{2+}$  channels. *Neuron* 31: 35–45, 2001.
  13. **Klug MG, Soonpaa MH, Koh GY, and Field LJ.** Genetically selected cardiomyocytes from differentiating embryonic stem cells form stable intracardiac grafts. *J Clin Invest* 98: 216–224, 1996.
  14. **Lee JH, Daud AN, Cribbs LL, Lacerda AE, Pereverzev A, Klockner U, Schneider T, and Perez-Reyes E.** Cloning and expression of a novel member of the low voltage-activated T-type calcium channel family. *J Neurosci* 19: 1912–1921, 1999.
  15. **Lee JH, Gomora JC, Cribbs LL, and Perez-Reyes E.** Nickel block of three cloned T-type calcium channels: low concentrations selectively block  $\alpha 1H$ . *Biophys J* 77: 3034–3042, 1999.
  16. **Leuranguer V, Monteil A, Bourinet E, Dayanithi G, and Nargeot J.** T-type calcium currents in rat cardiomyocytes during postnatal development: contribution to hormone secretion. *Am J Physiol Heart Circ Physiol* 279: H2540–H2548, 2000.
  17. **Maltsev VA, Rohwedel J, Hescheler J, and Wobus AM.** Embryonic stem cells differentiate in vitro into cardiomyocytes representing sinusnodal, atrial and ventricular cell types. *Mech Dev* 44: 41–50, 1993.
  18. **Maltsev VA, Wobus AM, Rohwedel J, Bader M, and Hescheler J.** Cardiomyocytes differentiated in vitro from embryonic stem cells developmentally express cardiac-specific genes and ionic currents. *Circ Res* 75: 233–244, 1994.
  19. **Nuss HB and Houser SR.** T-type  $Ca^{2+}$  current is expressed in hypertrophied adult feline left ventricular myocytes. *Circ Res* 73: 777–782, 1993.
  20. **Nuss HB and Marban E.** Electrophysiological properties of neonatal mouse cardiac myocytes in primary culture. *J Physiol* 479: 265–279, 1994.
  21. **Perez-Reyes E.** Molecular physiology of low-voltage-activated T-type calcium channels. *Physiol Rev* 83: 117–161, 2003.
  22. **Perez-Reyes E, Cribbs LL, Daud A, Lacerda AE, Barclay J, Williamson MP, Fox M, Rees M, and Lee JH.** Molecular characterization of a neuronal low-voltage-activated T-type calcium channel. *Nature* 391: 896–900, 1998.
  23. **Piedras-Renteria ES, Chen CC, and Best PM.** Antisense oligonucleotides against rat brain  $\alpha 1E$  DNA and its atrial homologue decrease T-type calcium current in atrial myocytes. *Proc Natl Acad Sci USA* 94: 14936–14941, 1997.
  24. **Pignier C and Potreau D.** Characterization of nifedipine-resistant calcium current in neonatal rat ventricular cardiomyocytes. *Am J Physiol Heart Circ Physiol* 279: H2259–H2268, 2000.
  25. **Qu Y and Boutjdir M.** Gene expression of SERCA2a and L- and T-type Ca channels during human heart development. *Pediatr Res* 50: 569–574, 2001.
  26. **Robbins J, Gulick J, Sanchez A, Howles P, and Doetschman T.** Mouse embryonic stem cells express the cardiac myosin heavy chain genes during development in vitro. *J Biol Chem* 265: 11905–11909, 1990.
  27. **Seisenberger C, Specht V, Welling A, Platzer J, Pfeifer A, Kuhbandner S, Striessnig J, Klugbauer N, Feil R, and Hofmann F.** Functional embryonic cardiomyocytes after disruption of the L-type  $\alpha 1C$  ( $Ca_v1.2$ ) calcium channel gene in the mouse. *J Biol Chem* 275: 39193–39199, 2000.
  28. **Sen L and Smith TW.** T-type  $Ca^{2+}$  channels are abnormal in genetically determined cardiomyopathic hamster hearts. *Circ Res* 75: 149–155, 1994.
  29. **Serrano JR, Perez-Reyes E, and Jones SW.** State-dependent inactivation of the  $\alpha 1G$  T-type calcium channel. *J Gen Physiol* 114: 185–201, 1999.
  30. **Viatchenko-Karpinski S, Fleischmann BK, Liu Q, Sauer H, Gryshchenko O, Ji GJ, and Hescheler J.** Intracellular  $Ca^{2+}$  oscillations drive spontaneous contractions in cardiomyocytes during early development. *Proc Natl Acad Sci USA* 96: 8259–8264, 1999.
  31. **Wobus AM, Rohwedel J, Maltsev V, and Hescheler J.** Development of cardiomyocytes expressing cardiac-specific genes, action potentials, and ionic channels during embryonic stem cell-derived cardiogenesis. *Ann NY Acad Sci* 752: 460–469, 1995.
  32. **Xu X and Best PM.** Postnatal changes in T-type calcium current density in rat atrial myocytes. *J Physiol* 454: 657–672, 1992.
  33. **Xu XP and Best PM.** Increase in T-type calcium current in atrial myocytes from adult rats with growth hormone-secreting tumors. *Proc Natl Acad Sci USA* 87: 4655–4659, 1990.
  34. **Yang HT, Tweedie D, Wang S, Guia A, Vinogradova T, Bogdanov K, Allen PD, Stern MD, Lakatta EG, and Boheler KR.** The ryanodine receptor modulates the spontaneous beating rate of cardiomyocytes during development. *Proc Natl Acad Sci USA* 99: 9225–9230, 2002.
  35. **Zhang Y, Cribbs LL, and Satin J.** Arachidonic acid modulation of  $\alpha 1H$ , a cloned human T-type calcium channel. *Am J Physiol Heart Circ Physiol* 278: H184–H193, 2000.
  36. **Zhang YM, Hartzell C, Narlow M, and Dudley SC Jr.** Stem cell-derived cardiomyocytes demonstrate arrhythmic potential. *Circulation* 106: 1294–1299, 2002.
  37. **Zhou Z and Lipsius SL.** T-type calcium current in latent pacemaker cells isolated from cat right atrium. *J Mol Cell Cardiol* 26: 1211–1219, 1994.